On the quasiparticle nature of the Bose polaron at finite temperature

UPC Seminar

Gerard Pascual López

Universitat Politècnica de Catalunya

July 6, 2021

Outline

Polaron system

- The polaron problem consists in a single impurity immersed in a Fermi or Bose bath.
- The first theoretical formulation of the problem backs to Landau and Pekar [1] who proposed the idea of quasiparticle.
- The Fermi polaron was studied the first due to the experimental achievement of Feshbach resonance.
- The Bose polaron offers the stimulating opportunity of studying the physics of the impurity in a bath that suffers a phase transition from a superfluid to a normal gas.

Bose polaron

- Different approaches at zero temperature have been considered: renormalization group theory [2], quantum Monte Carlo [3, 4, 5], variational methods [6, 7, 8, 9, 10, 11], and diagrammatic approaches [12].

- Including temperature in the previous theoretical approaches is difficult.

- There are studies that are only valid at low temperatures [13]. Other analysis show conflicting results [14, 15].

- Recent experiments studied this system at different temperatures claiming that the quasiparticle picture disappears [16].

Model

The Hamiltonian of a mobile impurity surrounded by a bath of N bosons at temperature T is described as follows,

$$H = -\frac{\hbar^2}{2m_B}\sum_{i=1}^{N}\nabla_i^2 - \frac{\hbar^2}{2m_I}\nabla_I^2 + \\ + \sum_{i<j} V_B(r_{ij}) + \sum_{i=1}^{N} V_I(r_{iI}) \ , \tag{1}$$

where m_B and m_I are the mass of the boson bath particles and of the impurity I.

Mathematical formalism of PIMC I

The density matrix that has to be solved is,

$$\mathscr{P}(|\phi_i\rangle) = \frac{1}{Z}e^{-\beta E_i} \quad \Longrightarrow \quad \hat{\rho} = \frac{e^{-\beta \hat{H}}}{Z}. \tag{2}$$

The density matrix can be redefined without the normalisation constant Z and projected onto the space basis,

$$\rho(\boldsymbol{R_1}, \boldsymbol{R_2}) = \langle \boldsymbol{R_1} | \hat{\rho} | \boldsymbol{R_2} \rangle = \langle \boldsymbol{R_1} | e^{-\beta \hat{H}} | \boldsymbol{R_2} \rangle \,, \tag{3}$$

where $\boldsymbol{R_i} = \{\boldsymbol{r_{1,i}}, \boldsymbol{r_{2,i}}, \cdots, \boldsymbol{r_{N,i}}\}$ is a set of space coordinates of the N particles of the system.

Mathematical formalism of PIMC II

Feynman came up with the following idea,

$$\hat{\rho} = e^{-\beta\hat{H}} = e^{-\varepsilon\hat{H}} \cdot e^{-\varepsilon\hat{H}} \cdot e^{-\varepsilon\hat{H}} \quad \cdots \quad e^{-\varepsilon\hat{H}} = \\ = \hat{\rho}_\varepsilon \cdot \hat{\rho}_\varepsilon \cdot \hat{\rho}_\varepsilon \quad \cdots \quad \hat{\rho}_\varepsilon, \tag{4}$$

where $\varepsilon = \beta/M$ and M is an arbitrary integer [17].

Projecting onto different space basis,

$$\rho(\boldsymbol{R_1}, \boldsymbol{R_{M+1}}; \beta) = \int d\boldsymbol{R_2} \cdots d\boldsymbol{R_M} \langle \boldsymbol{R_1} | \hat{\rho_\varepsilon} | \boldsymbol{R_2} \rangle \langle \boldsymbol{R_2} | \hat{\rho_\varepsilon} | \boldsymbol{R_3} \rangle \cdots \langle \boldsymbol{R_M} | \hat{\rho_\varepsilon} | \boldsymbol{R_{M+1}} \rangle = \\ = \int d\boldsymbol{R_2} \cdots d\boldsymbol{R_M} \rho(\boldsymbol{R_1}, \boldsymbol{R_2}; \varepsilon) \rho(\boldsymbol{R_2}, \boldsymbol{R_3}; \varepsilon) \cdots \rho(\boldsymbol{R_M}, \boldsymbol{R_{M+1}}; \varepsilon). \tag{5}$$

Approximations to decouple the density matrix I

The Chin approximation (CA) approaches the exponential of the Hamiltonian as a fourth-order action [18],

$$e^{-\varepsilon \hat{H}} \simeq e^{-\nu_1 \varepsilon \hat{W}_{a_1}} e^{-t_1 \varepsilon \hat{K}} e^{-\nu_2 \varepsilon \hat{W}_{1-2a_1}} e^{-t_1 \varepsilon \hat{K}} e^{-\nu_1 \varepsilon \hat{W}_{a_1}} e^{-2t_0 \varepsilon \hat{K}}. \qquad (6)$$

The resulting density matrix is the following,

$$\begin{aligned} \rho_{CA}(\boldsymbol{R}_1, \boldsymbol{R_2}; \varepsilon) = & \left(\frac{m}{2\pi\hbar^2\varepsilon}\right)^{9N/2} \left(\frac{1}{2t_1^2 t_0}\right)^{3N/2} \int d\boldsymbol{R}_{1A}\boldsymbol{R}_{1B} \exp\Bigg[\\ & - \frac{1}{4\lambda\varepsilon} \sum_{i=1}^{N} \left(\frac{1}{t_1}(\boldsymbol{r}_{i,1} - \boldsymbol{r}_{i,1A})^2 + \frac{1}{t_1}(\boldsymbol{r}_{i,1A} - \boldsymbol{r}_{i,1B})^2 + \frac{1}{2t_0}(\boldsymbol{r}_{i,1B} - \boldsymbol{r}_{i,2})^2 \right) \\ & - \varepsilon \sum_{i<j}^{N} \left(\frac{\nu_1}{2} V(r_{ij,1}) + \nu_2 V(r_{ij,1A}) + \nu_1 V(r_{ij,1B}) + \frac{\nu_1}{2} V(r_{ij,2}) \right) \\ & - 2\varepsilon^3 u_0 \lambda \sum_{i=1}^{N} \left(\frac{a_1}{2} |\boldsymbol{F}_{i,1}|^2 + (1-2a_1)|\boldsymbol{F}_{i,1A}|^2 + a_1 |\boldsymbol{F}_{i,1B}|^2 + \frac{a_1}{2}|\boldsymbol{F}_{i,2}|^2 \right) \Bigg]. \end{aligned} \qquad (7)$$

Boundary conditions

- Diagonal properties i.e. $\rho(\boldsymbol{R}, \boldsymbol{R}; \beta) \Longrightarrow \boldsymbol{R}_1 = \boldsymbol{R}_{M+1}$.
- Bosons particles $\Longrightarrow$ the density matrix is symmetric under permutations of $\{\boldsymbol{R}_1, \cdots, \boldsymbol{R}_M\}$,

$$\boldsymbol{R}_{M+1} = \mathcal{P}\boldsymbol{R}_1, \tag{8}$$

where $\mathcal{P}$ is a permutation of the particles,

$$\{\boldsymbol{r}_{1,M+1}, \boldsymbol{r}_{2,M+1}, \cdots, \boldsymbol{r}_{N,M+1}\} = \{\boldsymbol{r}_{1,p(1)}, \boldsymbol{r}_{2,p(2)}, \cdots, \boldsymbol{r}_{N,p(N)}\}, \tag{9}$$

where $p(i)$ is the label of the particle that is in permutation with the $i - th$ atom.

Implementation of PIMC method

Calculating previous integral using Monte Carlo method, with probability $p(\boldsymbol{R}_1, \cdots, \boldsymbol{R}_M)$

$$p(\boldsymbol{R}_1, \cdots, \boldsymbol{R}_M) = \prod_{i=1}^{M} \rho_{CA}(\boldsymbol{R}_i, \boldsymbol{R}_{i+1}; \varepsilon). \tag{10}$$

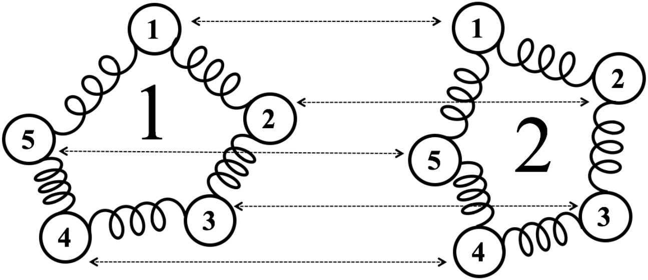

Figure: Representation of the interaction between two particles.

The *worm algorithm*

The new boundary conditions is now $R_{M+1} = \mathcal{P} R_1$

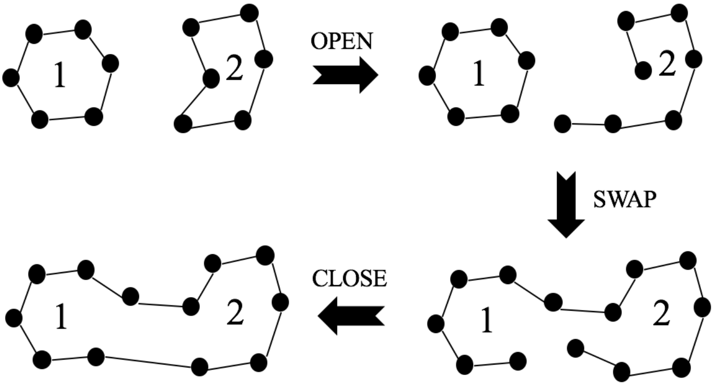

Figure: Representation of the permutation sampling using the *worm algorithm*.

Potentials

- Repulsive potential

$$V_{IB}(r) \propto \frac{1}{r^{12}}$$

- Attractive potential

$$V_{IB}(r) = -\alpha^2 \frac{\lambda(\lambda-1)}{\cosh^2(r\alpha)},$$

where the scattering length b,

$$b\alpha = \frac{1}{\lambda} - \frac{\pi}{2}\cot(\frac{\pi\lambda}{2}) + \sum_{n=1}^{\infty}\left(\frac{1}{\lambda+n} - \frac{1}{n}\right).$$

Delocalization of particles

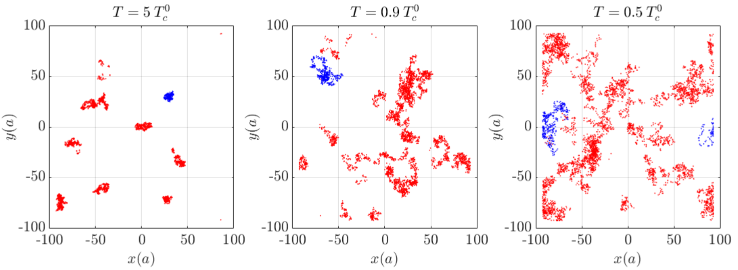

Figure: Projection of the positions of the particles in $2D$ at different temperatures.

Polaron Energy

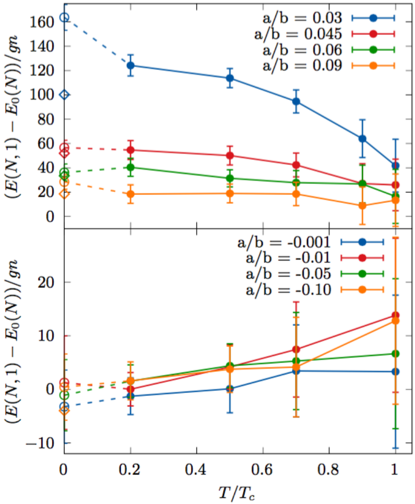

Figure: Polaron energy as a function of temperature ($na^3 = 10^{-4}$).

Effective mass and correlation functions

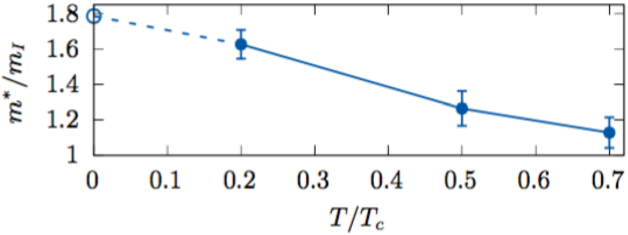

Figure: Effective mass of the Bose polaron as a function of temperature for a system with $a/b = 0.06$ and $na^3 = 10^{-5}$. The empty circle corresponds to data computed using quantum Monte Carlo methods at $T = 0\,T_c$ [3].

Fraction of condensed bosons

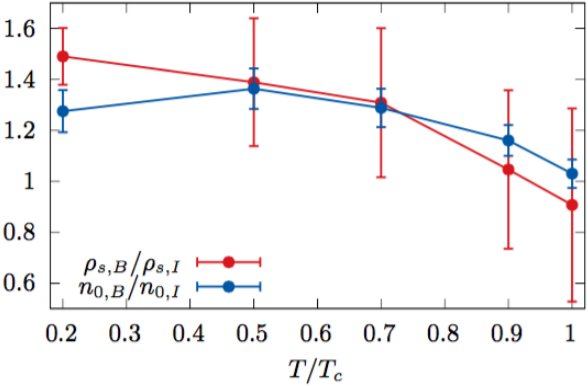

Figure: *Blue*: Ratio of the fraction of condensed bosons between a bath system ($n_{0,B}$) and an impurity system ($n_{0,I}$) at $a/b = 0.03$ and $na^3 = 10^{-4}$. *Red*: Ratio of the superfluid density between a bath system ($\rho_{s,B}$) and an impurity system ($\rho_{s,I}$) at the same conditions.

Quasiparticle Behaviour

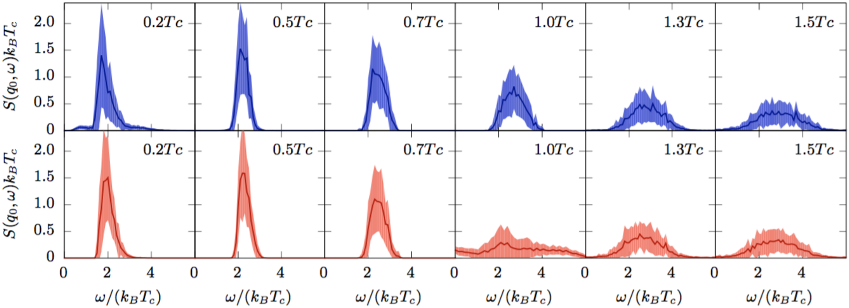

Figure: Dynamic structure factor as a function of temperature at $q_0a = 0.16$.

Conclusions

- We see similar trends for weak interactions in the attractive branch and also a particular asymmetry between the attractive and the repulsive branches.
- We see a competition between the bath, that tries to condensate all the particles, and the impurity that (slightly) hinders this condensation due to its interaction with the bath.
- Finally, we agree with [16] that the quasiparticle picture vanishes close to the critical temperature since we see that the effective mass tends to the bare mass when the temperature increases.

L. D. Landau and S. I. Pekar. “Effective mass of a Polaron”. In: *Zh. Eksp. Teor. Fiz* 18 (1948), pp. 419–423.

F. Grusdt et al. “Strong-coupling Bose polarons in a Bose-Einstein condensate”. In: *Phys. Rev. A* 96 (1 July 2017), p. 013607. DOI: 10.1103/PhysRevA.96.013607. URL: https://link.aps.org/doi/10.1103/PhysRevA.96.013607.

L. A. Peña Ardila and S. Giorgini. “Impurity in a Bose-Einstein condensate: Study of the attractive and repulsive branch using quantum Monte Carlo methods”. In: *Phys. Rev. A* 92 (3 Sept. 2015), p. 033612. DOI: 10.1103/PhysRevA.92.033612. URL: https://link.aps.org/doi/10.1103/PhysRevA.92.033612.

L. A. Peña Ardila and S. Giorgini. “Bose polaron problem: Effect of mass imbalance on binding energy”. In: *Phys. Rev. A* 94 (6 Dec. 2016), p. 063640. DOI: 10.1103/PhysRevA.94.063640. URL: https://link.aps.org/doi/10.1103/PhysRevA.94.063640.

L. A. Peña Ardila, G. E. Astrakharchik, and S. Giorgini. “Strong coupling Bose polarons in a two-dimensional gas”. In: *Phys. Rev. Research* 2 (2 June 2020), p. 023405. DOI: 10.1103/PhysRevResearch.2.023405. URL: https://link.aps.org/doi/10.1103/PhysRevResearch.2.023405.

Weiran Li and S. Das Sarma. “Variational study of polarons in Bose-Einstein condensates”. In: *Phys. Rev. A* 90 (1 July 2014), p. 013618. DOI: 10.1103/PhysRevA.90.013618. URL: https://link.aps.org/doi/10.1103/PhysRevA.90.013618.

Jesper Levinsen, Meera M. Parish, and Georg M. Bruun. "Impurity in a Bose-Einstein Condensate and the Efimov Effect". In: *Phys. Rev. Lett.* 115 (12 Sept. 2015), p. 125302. DOI: 10.1103/PhysRevLett.115.125302. URL: https://link.aps.org/doi/10.1103/PhysRevLett.115.125302.

Shuhei M. Yoshida et al. "Universality of an Impurity in a Bose-Einstein Condensate". In: *Phys. Rev. X* 8 (1 Feb. 2018), p. 011024. DOI: 10.1103/PhysRevX.8.011024. URL: https://link.aps.org/doi/10.1103/PhysRevX.8.011024.

Yulia E. Shchadilova et al. "Quantum Dynamics of Ultracold Bose Polarons". In: *Phys. Rev. Lett.* 117 (11 Sept. 2016), p. 113002. DOI: 10.1103/PhysRevLett.117.113002. URL: https://link.aps.org/doi/10.1103/PhysRevLett.117.113002.

- Moritz Drescher, Manfred Salmhofer, and Tilman Enss. "Real-space dynamics of attractive and repulsive polarons in Bose-Einstein condensates". In: *Phys. Rev. A* 99 (2 Feb. 2019), p. 023601. DOI: 10.1103/PhysRevA.99.023601. URL: https://link.aps.org/doi/10.1103/PhysRevA.99.023601.
- Senne Van Loon, Wim Casteels, and Jacques Tempere. "Ground-state properties of interacting Bose polarons". In: *Phys. Rev. A* 98 (6 Dec. 2018), p. 063631. DOI: 10.1103/PhysRevA.98.063631. URL: https://link.aps.org/doi/10.1103/PhysRevA.98.063631.
- Steffen Patrick Rath and Richard Schmidt. "Field-theoretical study of the Bose polaron". In: *Phys. Rev. A* 88 (5 Nov. 2013), p. 053632. DOI: 10.1103/PhysRevA.88.053632. URL: https://link.aps.org/doi/10.1103/PhysRevA.88.053632.

David Dzsotjan, Richard Schmidt, and Michael Fleischhauer. "Dynamical Variational Approach to Bose Polarons at Finite Temperatures". In: *Phys. Rev. Lett.* 124 (22 June 2020), p. 223401. DOI: 10.1103/PhysRevLett.124.223401. URL: https://link.aps.org/doi/10.1103/PhysRevLett.124.223401.

Nils-Eric Guenther et al. "Bose Polarons at Finite Temperature and Strong Coupling". In: *Phys. Rev. Lett.* 120 (5 Feb. 2018), p. 050405. DOI: 10.1103/PhysRevLett.120.050405. URL: https://link.aps.org/doi/10.1103/PhysRevLett.120.050405.

Bernard Field, Jesper Levinsen, and Meera M. Parish. "Fate of the Bose polaron at finite temperature". In: *Phys. Rev. A* 101 (1 Jan. 2020), p. 013623. DOI: 10.1103/PhysRevA.101.013623. URL: https://link.aps.org/doi/10.1103/PhysRevA.101.013623.

Zoe Z. Yan et al. “Bose polarons near quantum criticality”. In: *Science* 368 (6487 Apr. 2020), pp. 190–194. ISSN: 10959203. DOI: 10.1126/science.aax5850. URL: http://science.sciencemag.org/.

Richard Feynman. *Statistical Mechanics*. Addison-Wesley, 1972.

Siu A. Chin and C. R. Chen. “Gradient symplectic algorithms for solving the Schrödinger equation with time-dependent potentials”. In: *The Journal of Chemical Physics* 117.4 (2002), pp. 1409–1415.

Primitive approximations to decouple the density matrix

Using Baker–Campbell–Hausdorff formula,

$$\hat{\rho}_\varepsilon = e^{-\varepsilon(\hat{K}+\hat{V})} = e^{-\varepsilon\hat{K}} + e^{-\varepsilon\hat{V}} + e^{-\varepsilon\frac{1}{2}[\hat{K},\hat{V}]} + e^{-\varepsilon\frac{1}{12}[\hat{K},[\hat{K},\hat{V}]]} \dots \quad (11)$$

In the primitive approximation (PA), the commutator terms are not considered,

$$\begin{aligned}
\rho_{PA}(\boldsymbol{R_1}, \boldsymbol{R_2}; \varepsilon) &= \int d\boldsymbol{R'} \langle \boldsymbol{R_1} | e^{-\varepsilon\hat{K}} | \boldsymbol{R'} \rangle \langle \boldsymbol{R'} | e^{-\varepsilon\hat{V}} | \boldsymbol{R_2} \rangle = \\
&= \int d\boldsymbol{R'} (4\pi\lambda\varepsilon)^{-dN/2} e^{-\frac{(\boldsymbol{R_1}-\boldsymbol{R'})^2}{4\lambda\varepsilon}} e^{-\varepsilon V(\boldsymbol{R_2})} \delta(\boldsymbol{R'} - \boldsymbol{R_2}) = \\
&= (4\pi\lambda\varepsilon)^{-dN/2} e^{-\frac{(\boldsymbol{R_1}-\boldsymbol{R_2})^2}{4\lambda\varepsilon}} e^{-\varepsilon V(\boldsymbol{R_2})} \qquad (12)
\end{aligned}$$

Sampling subroutines in open and close configurations

- Translation
- Staging
- Cut
- Bind
- Move
- Swap

Properties computed

- Diagonal properties $\Longrightarrow$ Energy

$$\frac{E_V}{N} = \left\langle \frac{3}{2\beta} + \frac{1}{N}\sum_{j=1}^{M} \frac{(\boldsymbol{R}_{M+j} - \boldsymbol{R}_j)(\boldsymbol{R}_{M+j-1} - \boldsymbol{R}_{M+j})}{4\lambda\beta^2} + \right.$$
$$+ \frac{1}{2\beta N}\sum_{j=1}^{M}(\boldsymbol{R}_j - \boldsymbol{R}_j^C)\frac{\partial}{\partial \boldsymbol{R}_j}[U(\boldsymbol{R}_{j+1}, \boldsymbol{R}_j; \varepsilon) + U(\boldsymbol{R}_j, \boldsymbol{R}_{j-1}; \varepsilon)]$$
$$\left. + \frac{1}{MN}\sum_{j=1}^{M}\frac{\partial U(\boldsymbol{R}_{j+1}, \boldsymbol{R}_j; \varepsilon)}{\partial \varepsilon} \right\rangle. \quad (13)$$

- Off-diagonal properties

Generalisation of PIMC to two species of particles

1. Changes in the interaction between particles.
2. Particles of different species are distinguishable and, therefore, permutations can only be performed between particles of the same type.
3. There are two different worms.

Radial distribution function

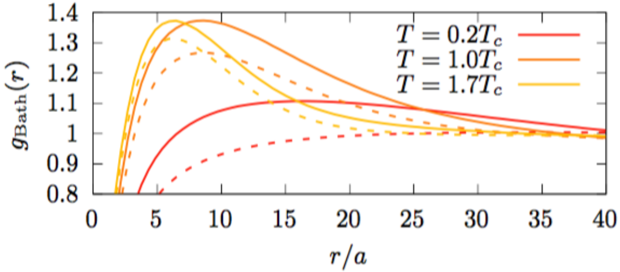

Figure: Radial distribution function of bath-bath particles at different temperatures ($a/b = 0.06$ and $na^3 = 10^{-4}$). Dashed lines correspond to systems without the impurity.